J Mater Sci (2007) 42:3603–3606
DOI 10.1007/s10853-006-0383-2

X-Ray diffraction and mössbauer spectra of nickel ferrite prepared by combustion reaction

**M. A. F. Ramalho · L. Gama · S. G. Antonio ·
C. O. Paiva-Santos · E. J. Miola ·
R. H. G. A. Kiminami · A. C. F. M. Costa**

Received: 2 May 2005 / Accepted: 1 May 2006 / Published online: 30 January 2007

Abstract Nickel ferrite powders with a nominal $NiFe_2O_4$ composition were synthesized by combustion reaction using urea as fuel. The powder was obtained using a vitreous silica basin heated directly on a hot plate at 480 °C until self-ignition occurred. After combustion, the powder was calcined at 700 °C for 2 h. The formation of the spinel phase and the distribution of cations in the tetrahedral and octahedral sites of the crystal structure were investigated by the Rietveld method, using synchrotron X-ray diffraction data and Mössbauer spectroscopy. The material presented a crystallite size of 120 nm and magnetic properties. The resulting stoichiometry after the Rietveld refinement was $(Fe_{0.989(2)}\ Ni_{0.011(2)})[Fe_{1.012(2)}\ Ni_{0.989(2)}]\ O_4$.

M. A. F. Ramalho · L. Gama · A. C. F. M. Costa
Department of Materials Engineering, Federal University of Campina Grande, 58109-970 Campina Grande, PB, Brazil

S. G. Antonio · C. O. Paiva-Santos
Department of Physical Chemistry, Institute of Chemistry, Paulista State University, 14800-900 Araraquara, SP, Brazil

E. J. Miola
Department of Physics, Federal University of São Carlos, 13565-905 São Carlos, SP, Brazil

R. H. G. A. Kiminami (✉)
Department of Materials Engineering, Federal University of São Carlos, 13565-905 São Carlos, SP, Brazil
e-mail: ruth@power.ufscar.br

Introduction

Nanostructured materials exhibit unusual physical and chemical properties that differ significantly from those of conventional bulk materials in terms of their extremely small size or large specific surface area [1–3]. Nickel ferrite, $NiFe_2O_4$, with an inverse spinel structure is used in electric and electronic devices and in catalysis. This material shows ferrimagnetism that originates from a magnetic moment of anti-parallel spins between Fe^{3+} ions at tetrahedral and octahedral sites and Ni^{2+} ions at octahedral sites [4].

The nickel ferrites with good magnetic properties are used in a wide variety of technological applications [5], including satellite communications, memory devices, computer components, antenna rods and transformer cores. Various preparation methods such as coprecipitation [6], hydrothermal synthesis [7], sol–gel [8], sonochemical preparation [9] and mechanical alloying [10] have been used to produce nickel ferrite nanoparticles. Among the various existing methods of chemical synthesis, combustion reaction is an alternative and promising technique for preparing soft ferrites, leading to highly pure, chemically homogeneous, nanometric scale particles [11–13].

The combustion reaction method is simple, involving a very fast chemical and exothermic reaction to form the material. The key characteristic of the process is that the heat required to trigger the reaction is supplied by the reaction itself instead of coming from an external source [11]. Metallic nitrates, which are the source of cations for the formation of metallic oxide, react with the fuel reducer, resulting in the formation of a fine, dry and usually crystalline powder oxide [14]. Apart from the aforementioned advantages, the combustion reaction method also has interesting characteristics such as its simplicity (since it does not require multiple stages), its relatively low cost, and the fact that it usually results in products with the desired structure and composition [15]. This paper reports on the structural characterization, by X-ray diffraction and Mössbauer spectroscopy, of nickel ferrite powders prepared by combustion reaction and calcined at 700 °C/2 h.

Experimental

Nanosize particle oxides of nickel ferrite with a nominal composition of $NiFe_2O_4$ were prepared by combustion reaction using urea as fuel. The materials employed were iron nitrate—$Fe(NO_3)_3 \cdot 9H_2O$ (Merck), nickel nitrate—$Ni(NO_3)_2 \cdot 6H_2O$ (Merck) and urea—$CO(NH_2)_2$ (Synth). Stoichiometric compositions of metal nitrate and urea were calculated, using the total oxidizing and reducing valences of the components, which serve as the numerical coefficients for the stoichiometric balance, so that the equivalence ratio Φ_c was unity and the energy released was maximum [13, 16]. The powder was prepared in a vitreous silica basin heated directly on a hot plate at 480 °C until self-ignition occurred. The resulting powder was calcined at 700 °C for 2 h to ensure complete crystallization of the ferrite phase.

The crystal structure of the calcined nickel ferrite powder was characterized by X-ray diffraction using synchrotron light data. The experimental setup consisted of a Si 111 double crystal monochromator with the first crystal refrigerated and the second sagitally curved. A scintillation detector was used. The monochromator was adjusted to select the energy of the absorption edge of Fe ($E = 7.1052$ keV, ($= 1.74487$ Å), so as to have a significant difference between the scattering factors of the Fe and Ni atoms. This energy allows one to refine the occupation of these ions to identify their distribution in the tetrahedral and octahedral sites. A Y_2O_3 sample was used as the standard to check the wavelength and instrumental broadening for a size-strain analysis. Rietveld refinements were performed to determine the cation distribution in the tetrahedral and octahedral sites in the material's crystal structure. The GSAS suite program [17] was used for the computations. The Thompson–Cox–Hastings pseudo–Voigt function was used as the profile function, with asymmetry corrected according to the formalism of Finger, Cox and Jephcroat [18]. During the refinements, only the profile parameters that varied with $\sec\theta$ and $\mathrm{tg}\theta$ were refined, since they can be related, respectively, to the crystallite size and microstrain ($\Delta d/d$). Crystallite size and microstrain analyses were made according to the equations described in the GSAS Manual [17].

The ^{57}Fe Mössbauer spectra, which were obtained at room temperature, were recorded at the Federal University of São Carlos, Brazil using an EG&G constant acceleration Mössbauer spectrometer in transmission mode. The source of nominal activity 15 mCi was ^{57}Co in an Rh matrix. Isomeric shifts were measured relative to the centroid of the α-Fe foil spectrum at room temperature. An α-Fe foil was also used to calibrate the velocity scale of the spectrometer. The Mössbauer data were fitted with a least-square program assuming a Lorentzian line shape.

Results

Figure 1 presents the Rietveld plot of the $NiFe_2O_4$ ferrite powder prepared by combustion reaction and calcined at 700 °C/2 h after refinement with the synchrotron data. The powder presented 100% of spinel phase nickel ferrite. The crystallite size of around 120 nm and an insignificant microstrain of about 1.2×10^{-5} (adimensional $\Delta d/d$ unit) were calculated from the refinement of the FWHM parameters.

The refinement of the site occupancies during the Rietveld refinement allowed us to determine the cation distribution in the tetrahedral and octahedral sites of the calcined material. To maintain the equilibrium of

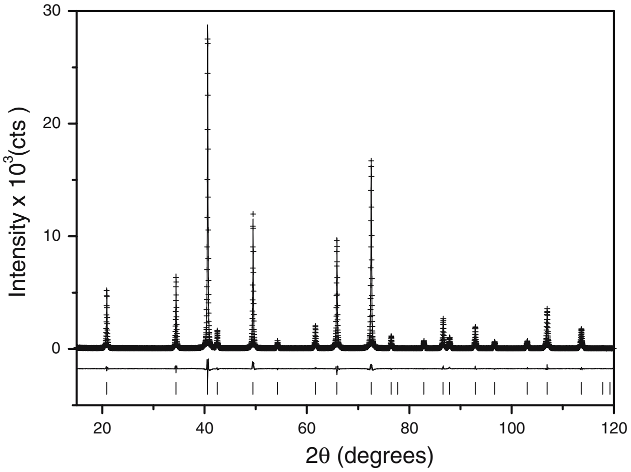

Fig. 1 Rietveld plot for the NF prepared through route NFC and calcined at 700 °C/2 h. The symbols "+" represents the observed diffractogram, the continuous line is the calculated diffractogram, and the continuous line below the observed and calculated diffractograms is the difference between them. The small vertical lines are the Bragg peak positions

the charge, a constraint was used whereby the increments in the occupancies of the cations in the octahedral site varied by half the occupancies of the cations in the tetrahedral sites. The resulting stoichiometry was:

$$(Fe_{0.989(2)}\ Ni_{0.011(2)})\ [Fe_{1.012(2)}\ Ni_{0.989(2)}]\ O_4$$

Other relevant refinement indices were: reduced $\chi^2 = 2.502$, Rwp = 9.62%, $RF^2 = 1.88\%$. Table 1 lists the data of the crystal. Where, χ^2 is the statistical agreement index calculated according the formulae given in the GSAS manual [17], page 166, $\chi^2 = M/(N - NP)$, where $M = \sum_i w_i(yo_i - yc_i)^2$, yo_i and yc_i are respectively the observed and calculated intensity at each step i, N is the number of observations and M is the number of parameters being refined.

Rwp = $M/\sum(\text{yoi})^2$, and RF^2 is $= [\sum(I_o - I_c)]/\sum I_o$, where I_o and I_c are respectively the observed and calculated intensity of the Bragg reflections.

Our XRD results were corroborated by Mössbauer spectroscopy (MS), revealing the presence of a single phase of the inverse spinel of nickel ferrite, and the formation of fine particles with a crystallite size of 120 nm after calcination of the $NiFe_2O_4$ powder. This analysis is possible thanks to the ability of Mössbauer spectroscopy (MS) to identify a single atomic species and its high sensitivity to changes in the atomic configuration surrounding the ^{57}Fe isotope. MS measures hyperfine interactions, providing valuable and often unequaled information on iron species' magnetic and electronic states, local crystalline symmetry in Fe sites, and structural defects [19, 20] (Table 2).

Table 1 Crystal data for the spinel calcined at 700 °C/2 h

Formula sum	$Fe_{0.50}\ Ni_{0.25}\ O$
Formula weight	58.60
Crystal system	Cubic
Space group	F d –3 m (no. 227)
Unit cell dimensions	*a* = 8.3389(1) Å
Cell volume	579.86(1) $Å^3$
Z	32
Density, calculated	5.370 g/cm^3

Atomic coordinates and isotropic displacement parameters (in $Å^2$)

Atom	Wyck.	Occ.	*X*	*Y*	*Z*	*U*
FE1	8^a	0.989(2)	1/8	1/8	1/8	0.0029(2)
NI1	8^a	0.011(2)	1/8	1/8	1/8	0.0029(2)
FE2	16*d*	0.506(1)	1/2	½	1/2	0.0029(2)
NI1	16*d*	0.494(1)	1/2	½	1/2	0.0029(2)
O3	32*e*	1.000	*u*	*U*	*u*	0.0029(2)

u = 0.2559(1)

Interatomic distances (Å)

FE1/NI1—O3 (tetrahedral site)	1.891(1)
FE2/NI2—O3 (octahedral site)	2.037(1)

Figure 2 shows a Mössbauer spectrum, taken at ambient temperature, of the $NiFe_2O_4$ ferrite samples prepared by combustion reaction and calcined at 700 °C/2 h. Note the adjustment of the experimental spectrum formed by the overlapping of two components: two sextets corresponding to magnetic scattering. The isomeric deviations (δ) of 0.37 mm/s and 0.25 mm/s were congruent with the presence of Fe (III) in two different states [21, 22]. This ferrite displays two strong interactions of super exchange between Fe^{+3}–O–Fe^{+3} and Fe^{+3}–O–Ni^{+2} in the $NiFe_2O_4$ lattice, where ferric ions occupy the center of the octahedral oxygen and the tetrahedral oxygen in equal proportion [23], while Ni^{+2} ions occupy mainly octahedral sites. Hence, the material's particle size comprises ferrimagnetic domains that cause the levels of energy of the ^{57}Fe nucleus to separate. It is well known that the superparamagnetic state of ferrimagnetic particles with a grain size below the critical one varies due to fluctuations of the magnetic moment in the particle in response to thermal disturbances. Thus, the $NiFe_2O_4$ crystals of 120 nm size were ferrimagnetic at ambient temperature and their spectrum showed overlapping of two standard magnetic sextets corresponding, respectively, to iron atoms in octahedral sites (O) and in tetrahedral sites (T) in the $NiFe_2O_4$ lattice [21, 22, 24].

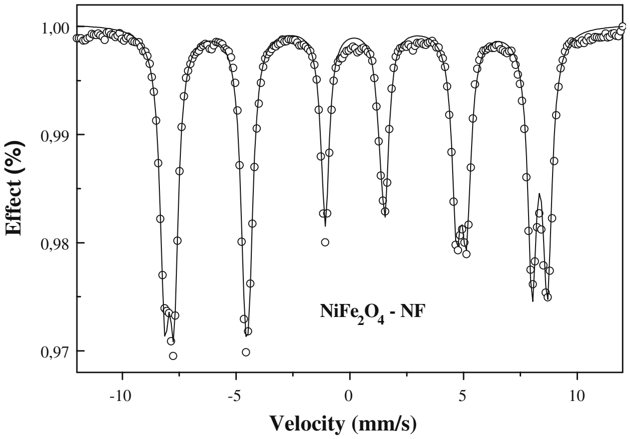

Fig. 2 Mössbauer spectrum, taken at ambient temperature, of the $NiFe_2O_4$ prepared by the method of combustion and calcined at 700 °C/2 h

Table 2 Results of the Mössbauer spectrum of ^{57}Fe of the sample of $NiFe_2O_4$

Samples	δ (mm/s)	Δ (mm/s)	Γ (mm/s)	H (kOe)	%	Phases
$NiFe_2O_4$	0.37	–	0.48	523	51	Octahedral
	0.25	–	0.46	489	49	Tetrahedral

δ, referring isomeric to the α-Fe; Δ, quadrupole scattering; Γ, full width at half maxima; H, magnetic hyperfine field

According to Shen et al. [25] and Kundig et al. [26], the absence of a magnetically split six-finger pattern, as was found in iron oxide calcined at 400 °C, indicates that the particles of iron species in the sample may be smaller than 10 nm. In the case of this work, the presence of patterns of six peaks representing magnetic scattering indicated that the $NiFe_2O_4$ powder particles were larger than 10 nm (the critical value causes variation of the superparamagnetic to the ferrimagnetic state).

Conclusions

The combustion reaction performed in a vitreous silica basin followed by calcination at 700 °C/2 h produced highly crystalline powders with a crystallite size of 120 nm. The Mössbauer spectrum of the $NiFe_2O_4$ ferrite sample at ambient temperature indicated that the ferrimagnetic interaction and the interfaces of the atomic states of a few crystallites (mudado por sugestão do revisor 3) were influenced by the combustion reaction preparation method. The Fe cations in the calcined material were distributed homogenously in the octahedral and tetrahedral sites, while the Ni cations were located mainly in the octahedral sites. The distribution of cations indicated that this was an inverse spinel with a $(Fe_{0.989(2)}\ Ni_{0.011(2)})\ [Fe_{1.012(2)}\ Ni_{0.989(2)}]\ O_4$ stoichiometry.

Acknowledgements The authors thank RENAMI, CNPq and FAPESP (Brazil) for their financial support of this work, and the National Laboratory of Synchrotron Light (LNLS), Campinas, Brazil for the XRD measurements.

References

1. Hayashi C (1987) Phys Today 40:44
2. Gleiter H (1989) Prog Mater Sci 33:223
3. Fendler JH (1987) Chem Rev 87:877
4. Kinemuchi Y, Ishizaka K, Suematsu H, Jiang W, Yatsui K (2002) Thin Solid Films 407:109
5. Visuanathan B, Murthy VRK (1990) Ferrites Materials Science and Technology, Nerosa Publishing House
6. Morrison AH, Haneda K (1981) J Appl Phys 52:2496
7. Komarnemi S, Fregeau E, Breval E, Roy R (1998) J Am Ceram Soc Commun 71:c–26
8. Courty Ph, Ajot H, Macilly Ch, Delmon B (1973) Powder Technol 7:21
9. Shafi KVPM, Koltypin Y, Gedanken A et al (1997) J Phys Chem B101:6409
10. Shi Y, Ding J, Liu X, Wang J (1999) J Magn Magn Mater 205:249
11. Costa ACFM, Tortella E, Morelli MR, Kiminami RHGA (2003) Mater Sci Forum 416–418:699
12. Costa ACFM, Tortella E, Morelli MR, Kaufman M, Kiminami RHGA (2002) J Mater Sci 37:3569
13. Costa ACFM, Tortella E, Morelli MR, Kiminami RHGA (2002) J Metas Nanocryst Mater 14:57
14. Zhang Y, Stangle GC (1994) J Mater Res 9(8):1997
15. Kiminami RHGA, Folz DC, Clarc DE (2000) Ceram Bull 70(3):63
16. Jain SR, Adiga KC, Pai Verneker V (1981) Combust Flame 40:71
17. Larson AC, Von Dreele RB (2004) General Structure Analysis System (GSAS). Los Alamos National Laboratory Report LAUR 86–748
18. Finger L,W Cox DE, Jephcoat AP (1994) J Appl Cryst 27:892, Stephens PJ (1998) Appl Cryst 32:281
19. Cohen L (1980) Application of Mössbauer spectroscopy, vol. II. Academic Press, New York
20. Brauer G, Matz W, Fetzer Cs (1990) Hyperfine Interact 56:1563
21. Halasa NA, DePasqual G, Drickamer HG (1974) Phys Rev B10(1):154
22. Sui Y, Su WH, Zheng FL, Xu DP (2000) Mater Sci Eng A 286:115
23. Anderson PW (1950) Phys Rev 79:350
24. Hartridge A, Bhattacharya AK, Sengupta M, Majumdar CK, Das D, Chintalapudi SN (1997) J Magn Magn Mater 176:L89
25. Tu M, Shen J, Chen Y (1997) Thermochimica Acta 302:117
26. Kundig W, Bommel H, Constabaris G, Lindquist RH (1996) Phys Rev B 142:327